# EPR spectroscopic investigation of radical-induced degradation of partially fluorinated aromatic model compounds for fuel cell membranes

Frank Schönberger,†*[a] Jochen Kerres,[a] Herbert Dilger[b] and Emil Roduner[b]
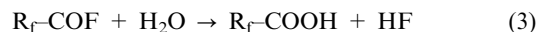
EPR spectroscopic investigations of reactions between monomeric model compounds representing typical structural moieties of poly(aryl) ionomers and photochemically generated hydroxyl radicals are reported. Deoxygenated solutions of the model compounds (in a water/methanol mixture) containing hydrogen peroxide at defined pH values were exposed to UV light in the flow cell within the cavity of an EPR spectrometer. Spectra were analyzed by computer simulation and the formed radicals were assigned by comparing their $g$-factors and hyperfine coupling constants (hfccs) with those from the literature and from density functional theory (DFT) calculations. The relevance for polymer electrolyte membrane fuel cells (PEMFCs) and alkaline-anion exchange membrane fuel cells (AAEMFCs) is discussed.

## 1. Introduction

Polymer electrolyte membrane fuel cells (PEMFCs) are—in principle—considered as promising energy conversion devices although many barriers are still in the way of their widespread commercialization. The most serious obstacles are the high system costs and the need for significant advances in hydrogen production and storage, as well as the performance and the durability of fuel cells under typical operating conditions. These conditions include extreme or cyclic change in load as well as the presence of impurities and inhomogeneities in the fuel and oxidant supply, the catatytic reaction, the proton conduction or the relative humidity.[1] Especially, the degradation of the membrane itself limits the lifetime of PEMFCs and needs to be fully understood on a molecular scale in order to minimize it by appropriate countermeasures. Besides physical and mechanical degradations (such as thinning and pinhole formation as a result of hydrolytic decomposition at elevated temperature and induced stresses),[2,3] membrane degradation by hydroxyl (HO•) and hydroperoxyl radicals (HOO•) is discussed in the literature.[2,4–8] HO• and HOO• are regular intermediates in the catalytic reduction of oxygen at the cathode[3,9] and might be responsible for membrane degradation after desorption from the catalyst surface.[8] Another often discussed source for the formation of HO• and HOO• is based on the evolution of small amounts of hydrogen peroxide as a side product,[6] especially at low coordinated platinum atoms (e.g. edge and corner atoms).[10,11] Hydrogen peroxide is mainly formed at the cathode side of the MEA but in principle it can

also be evolved at the anode side after oxygen has permeated through the membrane.[12] Although a certain percentage of the formed $H_2O_2$ might be washed out by the product water and the flowing gas, another fraction might diffuse into the membrane and decay into HO• by catalysis of bivalent metal ions at the elevated fuel cell operating temperature.[6]

For example, hydroxyl radicals are held responsible for initiating depolymerization starting at the carboxylic acid end groups of poly(perfluoroalkyl)sulfonic acids according to the following reactions (also known as backbone unzipping).[13]

$$R_f\text{–}CF_2COOH + HO^\bullet \rightarrow R_f\text{–}CF_2^\bullet + CO_2 + H_2O \quad (1)$$

$$R_f\text{–}CF_2^\bullet + {}^\bullet OH \rightarrow R_f\text{–}CF_2OH \rightarrow R_f\text{–}COF + HF \quad (2)$$

$$R_f\text{–}COF + H_2O \rightarrow R_f\text{–}COOH + HF \quad (3)$$

Such carboxylic acid endgroups are formed in the presence of water via perfluorocarbinol intermediates from sulfuric acid ester end-groups which result from the polymerisation initiator ($K_2S_2O_8$). More recent studies on the chemical stability of model compounds for perfluorinated sulfonic acid polymers also suggest side-chain scission and HO• radical attack of the sulfonic acid groups as possible degradation modes.[14,15]

The investigation of HO• and related radical induced degradation reactions of membranes and membrane building blocks by EPR spectroscopy has often been documented in the literature and recently reviewed by Schlick and Roduner.[16] Both in situ methods,[5,6,17] where an MEA is placed into a miniaturized fuel cell, and ex situ methods,[17,18] where the membrane is exposed to Fenton's reagent, hydrogen peroxide solution or vapor within the cavity of an EPR spectrometer, was applied. In order to get a molecular understanding of possible sites of attack for HO• and oxygen radicals in nonfluorinated poly(arylene ether) based ionomers a set of hydrogen peroxide containing aqueous solutions of monomeric model compounds was photolyzed within the cavity of the EPR spectrometer.[4,8,12,14,17] While these investigations were focussed on nonfluorinated aromatic[4,8,12,17] or fluorinated

[a] Institute of Chemical Process Engineering, University of Stuttgart, Böblinger Strasse 72, 70199 Stuttgart, Germany. E-mail: frankschoenberger@gmx.net; Fax: +49 (0)711 685 85 242; Tel: +49 (0)711 685 85 255
[b] Institute of Physical Chemistry, Pfaffenwaldring 55, 70569 Stuttgart, Germany. E-mail: e.roduner@ipc.uni-stuttgart.de; Fax: +49 (0)711 685 64 495; Tel: +49 (0)711 685 64 490
† Present address: Department of Chemistry and Biochemistry, University of South Carolina, 631 Sumter Street, Columbia, SC 29208, USA
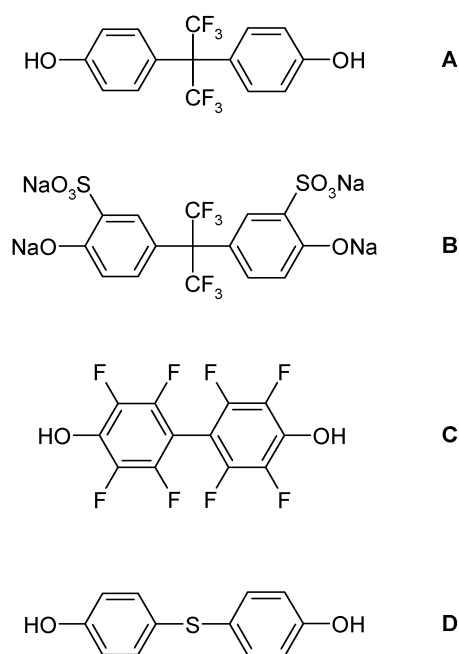
**Fig. 1** Overview of the investigated model compounds **A–D**.

non-aromatic[14] model compounds, the present contribution takes partially fluorinated poly(arylene ether) based ionomers into account.[19–32]

The model compounds **A** and **B** have $C_{sp^3}$–F bonds, **C** represents a poly(aryl) structure with $C_{sp^2}$–F bonds, and **D** is a widely used building block with a C–S–C bridge (cf. Fig. 1). Aromatic polymers with thioether instead of ether bridges in their backbone have also been discussed as PEM materials[33–35] which might be due to their oxidizabiliy to the sulfone group. Such an oxidation process could be effective as an 'internal antioxidant' and could prevent the ionomer from molecular weight degradation caused by radical induced processes up to a certain point.[36,37]

## 2. Experimental and theoretical methods

### 2.1 Sample preparation and EPR measurements

The model compounds **A–D** were exposed to HO• radicals and their reaction products with water and hydrogen peroxide, respectively (for details: cf. section: Overview of the reaction mixture) in a quartz flow cell (0.4 × 10 × 50 mm) within the cavity of a Varian E-Line X-Band EPR spectrometer. For this purpose deoxygenated methanolic–aqueous solutions or aqueous solutions of the model compound and hydrogen peroxide (with well-defined pH values) are circulated through the cavity by a syringe pump (with a constant flow rate which can be varied from 8 to 135 ml h$^{-1}$ and which corresponds to residence times in the flow cell between 90 and 5 s, respectively). Methanol was necessary as a cosolvent because of the hydrophobic nature of the nonsulfonated model compounds **A**, **C** and **D**. In order to exclude the existence of any solvent-derived radicals, control experiments without the model compound were carried out. A 500 W high-pressure mercury arc-lamp (Oriel 66142) focussed on the flow cell

initiates the photolytical cleavage of hydrogen peroxide into HO• radicals. Wavelengths below 210 nm and above 400 nm are absorbed by an appropriate filter solution (1.14 M NiSO$_4$; 0.21 M CoSO$_4$; 0.01 M H$_2$SO$_4$).[4] All measurements were carried out at room temperature.

The solutions were prepared from doubly distilled water and spectrophotometric grade methanol ($\geq$ 99.9%, Aldrich). The pH values of the solutions were adjusted with concentrated sulfuric acid and caustic potash solution, respectively, by using a digital WTW pH meter (model pH 330) calibrated with commercial buffer solutions. All the solutions were thoroughly deoxygenated by bubbling with nitrogen (for at least 15 min) before injection into the flow system.

Hydrogen peroxide solution (30%) was purchased from Merck and the model compounds **A**, **C** and **D** from Aldrich.

The model compound **B** was synthesized from **A** by electrophilic aromatic substitution as follows: 40.00 g (118.97 mmol) 2,2-bis(4-hydroxyphenyl)hexafluoropropane (**A**) and 80 ml concentrated sulfuric acid were stirred at 40 °C for 18 h. The reaction mixture was then poured onto ice cubes (ca. 200 g). After filtration, the product was precipitated by adding 300 g sodium chloride. Finally, it was recrystallized several times from methanol/water mixtures (9/1, v/v) and dried at 75 °C in a vacuum oven.

$^1$H NMR (250 MHz, D$_2$O, $\delta$): 7.83 (s, 1H), 7.41 (d, $^3J_{H–H}$ = 8.2 Hz, 1H); 7.06 (d, $^3J_{H–H}$ = 8.8 Hz, 1H). $^{13}$C NMR (50 MHz, D$_2$O, $\delta$): 156.87; 137.51; 132.09; 130.47; 126.60 (q, $^1J_{C–F}$ = 287 Hz); 126.28; 120.10; 65.75 (septet, $^2J_{C–F}$ = 25.7 Hz). Elemental analysis for C$_{15}$H$_6$O$_8$F$_6$S$_2$Na$_4$ {experimental (theoretical) values in [%]}: C: 31.23 (30.83); H: 2.04 (1.04); Cl: 0.85 (0.00).

The ratio between the concentrations of the model compound and of hydrogen peroxide was first estimated from their UV spectra in such a way that the main part of photons is absorbed by hydrogen peroxide according to the following inequation:

$$\varepsilon(H_2O_2) \times c(H_2O_2) \gg \varepsilon_i \times c_i \qquad (4)$$

Herein, $\varepsilon(H_2O_2)$ and $\varepsilon_i$ are the molar extinction coefficients of hydrogen peroxide and of the model compound $i$, $c(H_2O_2)$ and $c_i$ describe their concentrations. However, the extinction coefficients of the model compounds are relatively high compared to that of hydrogen peroxide (cf. for example: $\varepsilon(H_2O_2)$ = 98 M$^{-1}$ cm$^{-1}$; $\varepsilon_C$ = 3904 M$^{-1}$ cm$^{-1}$; $\varepsilon_A$ = 30 088 M$^{-1}$ cm$^{-1}$ at 230 nm and pH = 12; determined by UV spectroscopy) so that their concentrations must be significantly smaller than that of hydrogen peroxide.

Therefore, the final composition of the sample solutions was identified from preliminary EPR experiments in the presence and absence of hydrogen peroxide. The ideal concentration ratio was found when the EPR spectrum in the presence of hydrogen peroxide exhibits an optimal signal-to-noise-ratio while no or only minor EPR signals in the absence of hydrogen peroxide are detectable. Thus it can be assumed that the observed EPR signals in the presence of hydrogen peroxide primarily result from the reaction of HO• radicals with the model compound and that they are not caused by any solvent-derived radicals.

## 2.2 Analysis and interpretation of EPR spectra

The EPR spectra were analyzed by Microcal Origin® Version 7.0. Hyperfine coupling constants (hfcc) were derived from computer simulations using WINSIM®.[38] EPR signals were then assigned by comparing either with literature values[39] (if available for the expected radicals) or with the results of quantum mechanical calculations (using Gaussian 03).[40] Density functional theory (DFT) based on the unrestricted Kohn–Sham (UKS) methods[41] has often been used for the calculation of hyperfine coupling constants in the literature.[42–45] Primarily, the spin population $\rho(r_X)$ at the nucleus X is computed, which is proportional to the hyperfine coupling constant $a_X$ (the Fermi contact interaction):[46]

$$a_X = \frac{2\mu_0}{3}\left(\frac{g_e}{g}\right)g_X\beta_N\rho(r_X) \tag{5}$$

Herein, $g_e/g$ describes the ratio of the isotropic $g$-factors of the radical and of the electron (approximated with 1 in the DFT calculations), $\mu_0 = 4\pi \times 10^{-7}$ T$^2$ J$^{-1}$ m$^3$ is the vacuum permeability, $g_X$ is the nucleus $g$-factor of X and $\beta_N = 5.0508 \times 10^{-7}$ J T$^{-1}$ the nuclear magneton. The spin population $\rho(r_X)$ is computed as the expectation value of the spin operator $\hat{S}_z$ over the electronic wave function:

$$\rho(r_X) = S_z^{-1}\left\langle \psi \left| \sum_{\nu=1} \delta(r_\nu - r_X)\hat{S}_z(\nu) \right| \psi \right\rangle \tag{6}$$

$$= \rho^\alpha(r_\nu) - \rho^\beta(r_X)$$

The index $\nu$ runs over all electrons and $S_z$ is the quantum number which belongs to the projection of the total electron spin on the $z$ axis (1/2 for radicals). Any single point calculations in this work were done with the hybrid functional B3LYP[47–52] which turned out to be the most appropriate for the calculation of hyperfine coupling constants.[53] EPR-III[44,52] was used as a basis set if the corresponding radical only contained elements of the first two periods of the table of elements. For all the other radicals (e.g. with sulfur atoms) the basis sets 6-31G(d) and TZVP were applied.[42] These basis sets were used in all cases for the optimization of radical geometry before the single point calculations.

## 3. Results and discussion

### 3.1 Overview of the reaction mixture

According to eqn (4) the absorption of photons by $H_2O_2$ must be larger than that by the model compounds. Depending on the quantum yield a certain amount of hydroxyl radicals is formed by photolysis.

$$H_2O_2 \xrightarrow{h\nu} 2HO^\bullet \tag{7}$$

However, these HO$^\bullet$ radicals are only detectable at very low temperatures or indirectly by using spin traps (the same is true for O$^{\bullet-}$, HOO$^\bullet$ and O$_2^{\bullet-}$). The primarily formed HO$^\bullet$ radicals are highly reactive and can react with further hydrogen peroxide or solvent molecules or their dissociation products (HO$^-$, HOO$^-$), as well as with the aromatic model compounds. First of all, reactions of HO$^\bullet$ with $H_2O_2$, HOO$^-$, HO$^-$ and CH$_3$OH will be considered (cf. Table 1, Reactions a–d).

**Table 1** Rate constants for the reactions of HO$^\bullet$ with $H_2O_2$, $H_2O$ and CH$_3$OH and with its dissociation products. Values are taken from ref. 54–56 if not otherwise stated

| | pH | Reaction | Rate constant/ $10^9$ M$^{-1}$ s$^{-1}$ |
|---|---|---|---|
| a | 2–4 | HO$^\bullet$ + $H_2O_2$ → $H_2O$ + HOO$^\bullet$ | 0.042[57] |
| b | 7.7–13 | HO$^\bullet$ + HOO$^-$ → $H_2O$ + O$_2^{\bullet-}$ | 7.5 |
| c | 11.0 | HO$^\bullet$ + HO$^-$ → $H_2O$ + O$^{\bullet-}$ | 12 |
| d | 6–7 | HO$^\bullet$ + CH$_3$OH → $^\bullet$CH$_2$OH + $H_2O$ | 0.97[58] |
| | | HO$^\bullet$ + CH$_3$OH → CH$_3$O$^\bullet$ + $H_2O$ | |
| e | 13 | O$^{\bullet-}$ + HOO$^-$ → HO$^-$ + O$_2^{\bullet-}$ | 0.4 |
| f | 13.1–13.6 | O$^{\bullet-}$ + CH$_3$OH → $H_2O$ + $^\bullet$CH$_2$O$^-$ | 0.75 |
| g | 7.0 | HO$^\bullet$ + $^\bullet$OH → $H_2O_2$ | 5.5 |
| h | 2.74–6.75 | HO$^\bullet$ + O$_2^{\bullet-}$ → HO$^-$ + $^1O_2$ | 9.4 |
| i | >12 | HO$^\bullet$ + O$^{\bullet-}$ → HOO$^-$ | ≤20 |
| j | 13–14 | O$_2^{\bullet-}$ + O$^{\bullet-}$ + $H_2O$ → 2 HO$^-$ + $^1O_2$ | 0.6 |

They lead to the formation of further radical species like the oxygen radical anion (O$^{\bullet-}$), the hydroperoxyl radical (HOO$^\bullet$), and the superoxide radical anion (O$_2^{\bullet-}$). The course of the reaction strongly depends on the pH value in the solution and can be estimated qualitatively by means of the acid constants of the corresponding acid–base pairs $H_2O_2$/HOO$^-$ (p$K_a$ = 11.7),[8] HO$^\bullet$/O$^{\bullet-}$ (p$K_a$ = 11.5),[59] and HOO$^\bullet$/O$_2^{\bullet-}$ (p$K_a$ = 4.7),[60] as well as by means of the rate constants listed in Table 1. In the presence of CH$_3$OH that serves as a cosolvent for the nonsulfonated model compounds **A**, **C**, and **D**, hydroxymethyl ($^\bullet$CH$_2$OH) or methoxy radicals (CH$_3$O$^\bullet$) can be formed through H abstraction by HO$^\bullet$ radicals. In none of the cases reported here the hydroxymethyl radical, which is the reaction product of HO$^\bullet$ radicals with methanol, could be detected. If it was present, it could be distinguished easily from the intermediates observed because of its larger hyperfine coupling constant and lower $g$-values. In the absence or in case of a deficiency of methanol, HO$^\bullet$ radicals preferably react with $H_2O_2$ to HOO$^\bullet$ and with HOO$^-$ to O$_2^{\bullet-}$. The latter reactions proceed much faster in alkaline than in acid environment (reactions a and b). HO$^\bullet$ radicals abstract hydrogen from hydroxide ions in a diffusion-controlled reaction at pH > 11 (reaction c) and form the oxygen radical anion (O$^{\bullet-}$). At very high pH values (pH > 13), the concentration of O$^{\bullet-}$ is much larger than that of its corresponding acid (HO$^\bullet$) so that O$^{\bullet-}$ might be the reactive species (reactions e and f). Radical recombinations (such as reactions g to j) can also occur in the examined reaction solutions.

To summarize, it can be said that at pH < 10 the HO$^\bullet$ and HOO$^\bullet$ radicals are dominant, while at pH > 13 the O$^{\bullet-}$ and O$_2^{\bullet-}$ species exist predominantly. In the pH range 10 ≤ pH ≤ 13 the reaction solution consists of a complex mixture of HO$^\bullet$, O$^{\bullet-}$ and O$_2^{\bullet-}$. The concentration of HOO$^\bullet$ can be neglected in this range (p$K_a$(HOO$^\bullet$/O$_2^{\bullet-}$) = 4.7). Beside possible reactions of the aromatic model compounds with the four reactive species (HO$^\bullet$, O$^{\bullet-}$, HOO$^\bullet$, O$_2^{\bullet-}$) it has to be considered that they can be involved directly in any photophysical processes or photochemical reactions.[61]

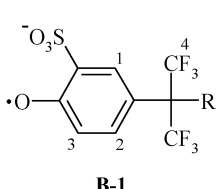### 3.2 2,2-Bis(4-hydroxyphenyl)hexafluoropropane (A)

Most of the EPR spectra recorded under various experimental conditions (different pH values [pH > 10.5, no signals were detectable below pH = 10.5], flow rates and concentration

ratios between **A** and $H_2O_2$) appear more or less chaotic, which makes a clear interpretation impossible. Therefore further examinations were carried out with the sulfonated form of **A** (*cf.* section 3.3) which also represents a typical structural moiety in partially fluorinated poly(arylene ether) based ionomers.[19,20,25]

### 3.3 Tetranatrium-3,3′(1,1,1,3,3,3-hexafluoropropane-2,2-diyl)bis(6-oxidobenzenesulfonate) (B)

The model compound **B** forms radicals under UV irradiation both in the absence and in the presence of $H_2O_2$ at pH = 9.45 (Fig. 2a and b). The singlet with g = 2.0033 observed under $H_2O_2$-free conditions could be assigned to the $^\bullet SO_3^-$ radical in good accordance with literature.[62] This radical is generated by direct photolysis of the C–S bond. The lack of the simultaneously formed phenyl radical indicates an extremely short lifetime of this species so that its stationary concentration might be below the detection limit of about $10^{-9}$ M.[63] In the presence of $H_2O_2$ the singlet caused by the $^\bullet SO_3^-$ radical disappears. Instead, another signal can be detected which is most probably caused by the phenoxyl radical **B-1** (*cf.* Fig. 2c.) and Table 2). Unfortunately, there are no g-factors and hyperfine coupling constants available in the literature for this radical. The structure assignment is thus based on a comparison with similar radicals[39] and with the



**Fig. 2** (a) Experimental EPR spectrum of **B** in the presence of 85 mM $H_2O_2$ at pH = 9.45 in aqueous solution under UV irradiation (12.8 mM **B**, pH = 9.45, flow rate 35 ml h$^{-1}$). (b) Control experiment under the same conditions, but in the absence of $H_2O_2$. (c) Simulation of the phenoxyl radical **B-1**.

**Table 2** EPR parameter of the radical **B-1** formed during the reaction of **B** with $H_2O_2$ under UV irradiation at pH = 9.45 and at a flow rate of 35 ml h$^{-1}$. Hyperfine coupling constants (hfcc) are taken from computer simulation using WINSIM and compared with values from DFT calculation results

| hfcc [G] from | | | |
|---|---|---|---|
| Simulation | DFT | g-Factor | Proposed structure[c] |
| 1 H (1): 1.43 | 1 H (1): 1.49[a] (1.52)[b] | 2.0048 | |
| 1 H (2): 3.74 | 1 H (2): 2.37[a] (2.39)[b] | | |
| 1 H (3): 0.58 | 1 H (3): 1.32[a] (1.30)[b] | | |
| 6 F (4): 0.85 | 6 F (4): 1.22[a] (1.20)[b] | | |



**B-1**

[a] B3LYP/TZVP//B3LYP/TZVP. [b] B3LYP/6-31G(d)//B3LYP/6-31G(d). [c] R = $C_6H_3$(m-$SO_3^-$)(p-$O^-$).

results of density functional theoretical calculations. Especially the radical geometry, electron correlation and the used basis set influence the quality of the theoretical prediction of EPR parameters in comparison to the experimental ones. In fact, the calculation of isotropic hyperfine coupling constants is one of the most demanding issues in theoretical chemistry.[42] The hyperfine coupling constant is proportional to the spin population (eqn (5)) which denotes the *difference* between the contributions due to electrons having spin α and β (eqn (6)). Small calculated hyperfine coupling constants always imply large relative errors as the calculated value is a small difference of two very high numbers. Here, the experimentally found values for the hyperfine coupling constants often lie in the range around 0 which explains the observed differences between the experimental and theoretical values. Furthermore, the size of the radical which consists of 37 atoms and the presence of sulfur complicate the absolute calculation of hyperfine coupling constants further.[44]

The formation of the phenoxyl radical **B-1** could be explained by reaction of the corresponding bisphenolate anion with HO$^\bullet$ radicals either by a one-electron mechanism or by an addition/elimination mechanism *via* a hydroxylcyclo-hexadienyl radical.[64,65] The lack of the latter (intermediate) radicals in the EPR spectra does not necessarily mean that they are not formed, but that their concentration might be below the detection limit. Therefore, no definite information on the formation mechanism of **B-1** can be given on the basis of these data.

Fig. 3 compares the EPR spectra of the model compound **B** at various pH values in the presence of $H_2O_2$ under UV irradiation. While no signals are detectable at very low pH values (pH = −0.80) under the chosen reaction conditions, there are additional small signals in the range between pH = 3.10 and 5.30 besides the singlet caused by the $^\bullet SO_3^-$. Although no reliable simulation of these signals was possible due to the poor signal-to-noise ratio, it can be supposed that they are caused by traces of **B-1**. In the pH range between pH = 7.3 and pH = 11.4, **B-1** seems to be the only species. The loss of hyperfine structure with increasing pH value is attributed to the presence of triplet oxygen ($^3O_2$) which causes spin
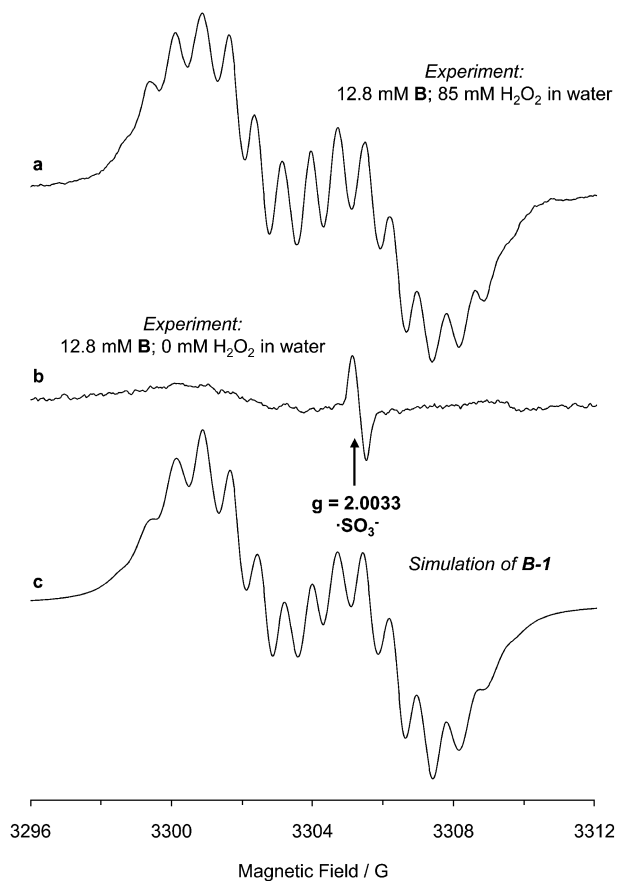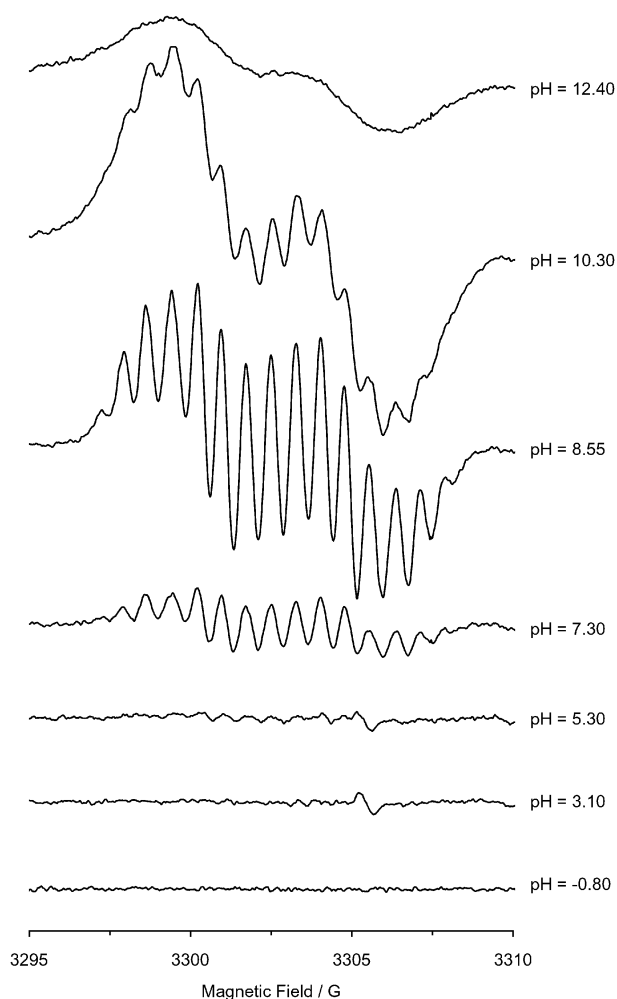
**Fig. 3** EPR signals of the model compound **B** in the presence of $H_2O_2$ (85 mM) under UV irradiation and in dependence of the pH value (conditions: 12.8 mM **B**; flow rate = 35 ml h$^{-1}$). Plain water was used as a solvent in all experiments.

exchange in the presence of any free radicals, leading to a dramatic line broadening.

Since all solutions were thoroughly deoxygenated before injecting into the EPR spectrometer triplet oxygen can only be formed *in situ*. This is also in accord with the observation of gas evolution in the sample cell especially at higher pH values. Oxygen bubbles out of the solution only when saturation is reached at a concentration of *ca.* 0.3 mM, which is higher than the concentration of any EPR active species in the solution. It is known from the literature that oxygen generated photo-chemically from hydrogen peroxide exists in a singlet state.[66,67] The lifetime of the so-formed singlet oxygen in water is reported to be 2 μs.[68] However, the residence time of the injected solution in the flow cell of the EPR spectrometer amounts to 20 s at a flow rate of 35 ml h$^{-1}$. A part of the evolved singlet oxygen might be embedded in the bubbles, where its lifetime is considerably higher than in water (7 to 12 s).[69] However, another part of the singlet oxygen might diffuse into the solution, transform into the triplet state, and cause the observed line broadening.

### 3.4 2,2′,3,3′,5,5′,6,6′-Octafluoro-4,4′-biphenol (C)

EPR signals (Fig. 4) could be detected under the chosen conditions both in an acidic ($0 \leq$ pH $\leq 3.5$) and a basic medium ($11 \leq$ pH $\leq 14$). While the signals detected at low pH values (pH $\leq 3.5$, depicted for pH = 0 in Fig. 4 as an example) are most probably generated by a photophysical or photochemical path, the signals at higher pH values might result from the reaction of HO• and related radicals with the model compound **C**. But first, the spectra in the absence of hydrogen peroxide will be discussed. A singlet with a very low g-factor (g = 2.0007) and a relatively low intensity is observed both at pH = 0 and at pH = 12. Definite structure assignments of the species responsible for this singlet cannot be given here. The energy of a photon emitted by the radiation source (in its maximum at 230 nm) would be sufficient for the homolytic cleavage of bonds with a maximum dissociation energy of *ca.* 520 kJ mol$^{-1}$. Thus a cleavage of any C–F bonds ($E_D$(C–F) = 477–644 kJ mol$^{-1}$)[70] or C–C bonds ($E_D$(C$_{ar}$–C$_{ar}$) $\approx$ 518 kJ mol$^{-1}$)[71] could be possible under these conditions. However, fluorine atoms formed by photolysis of any C–F bonds might react further with water (eqn (8)).[72]

$$F^• + H_2O \rightarrow HF + HO^• \qquad (8)$$

Although the low g-factor of 2.0007 argues for a σ radical, it is rather unlikely that the signal is caused by a perfluorinated phenyl radical (according to reaction (1) or (2) in Fig. 5), since one should expect further hyperfine splittings due to the remaining fluorine atoms. However, it cannot be excluded that such radicals might be present as very short-lived intermediates since their spin concentration could be below the detection limit of the EPR spectrometer. Eventually, the singlet at g = 2.0007 could be explained by a photoisomerization of one of the perfluorinated benzene rings to the corresponding Dewar benzene ring (reactions (3) and (4) in Fig. 5) which passes through an EPR active intermediate.[73–75]
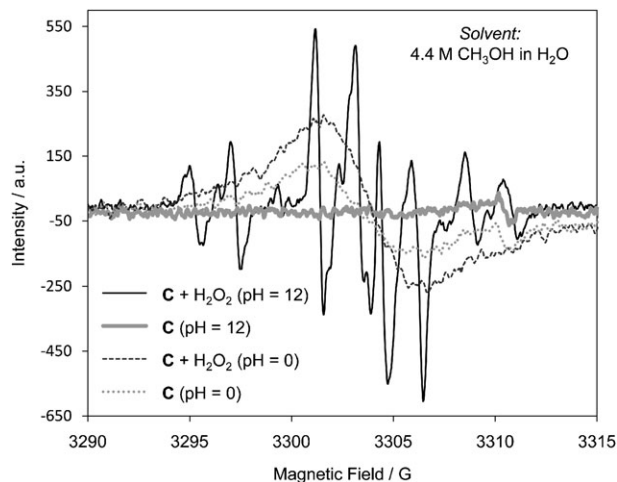


**Fig. 4** EPR spectra of the model compound **C** (4.4 mM **C**, 85 mM $H_2O_2$ in acidic (flow rate: 10 ml h$^{-1}$) and alkaline (flow rate: 55 ml h$^{-1}$) methanolic–aqueous solutions (4.4 M CH$_3$OH) (recorded with the same modulation amplitude of 0.4 G).
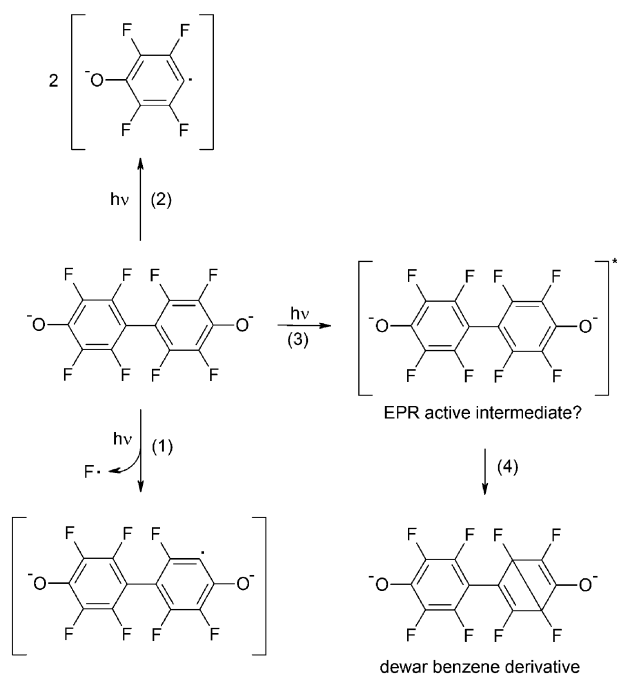
**Fig. 5** Possible photolytic cleavage of **C** (reactions (1) and (2) and photoisomerization to the corresponding dewar benzene derivative *via* excited (possibly EPR active) intermediates (reactions (3) and (4)).

The photolytic cleavage-off of F$^{\bullet}$ and the subsequent formation of HO$^{\bullet}$ according to eqn (8) could also be the reason for the similar EPR signals of **C** at pH = 0 both in the absence and in the presence of hydrogen peroxide (*cf.* **C** (pH = 0) and **C** + H$_2$O$_2$ (pH = 0) in Fig. 4). At this pH value, the addition of HO$^{\bullet}$ radicals to **C** under the formation of hydroxycyclohexadienyl radicals with subsequent HF elimination should be expected. Unfortunately, the EPR signals of **C** (pH = 0) and **C** + H$_2$O$_2$ (pH = 0) could not be resolved further and thus no details on possible hyperfine coupling constants could be revealed.

When the pH value is increased above pH = 3.5, the signals disappear. Only above pH = 11 are other signals detectable in the presence of hydrogen peroxide under UV irradiation (**C** + H$_2$O$_2$ (pH = 12) in Fig. 4). In the absence of hydrogen peroxide, however, only the narrow singlet at $g$ = 2.0007 can be observed (**C** (pH = 12) in Fig. 4). As depicted in Fig. 6 and summarized in Table 3 the EPR spectrum in the presence of hydrogen peroxide could be interpreted as a superposition of several fluorinated radicals of the phenoxyl and benzosemiquinone type.

The experimental EPR spectrum of **C** is shown again in Fig. 6a and compared with the simulated superposition of the radicals **C-1** to **C-5** (*cf.* Fig. 6b–g and Table 3) which may be considered as the key contribution. However, the experimental spectrum in Fig. 6a clearly contains further species to a minor extent. When the experimental (Fig. 6a) and the simulated (Fig. 6b) spectra are compared, it is obvious that the outer part of the simulated spectrum does not match very well the experimental one. Although a definite conclusion cannot be drawn at this point because of the low intensity of any minor radical species, the EPR pattern is compatible with the
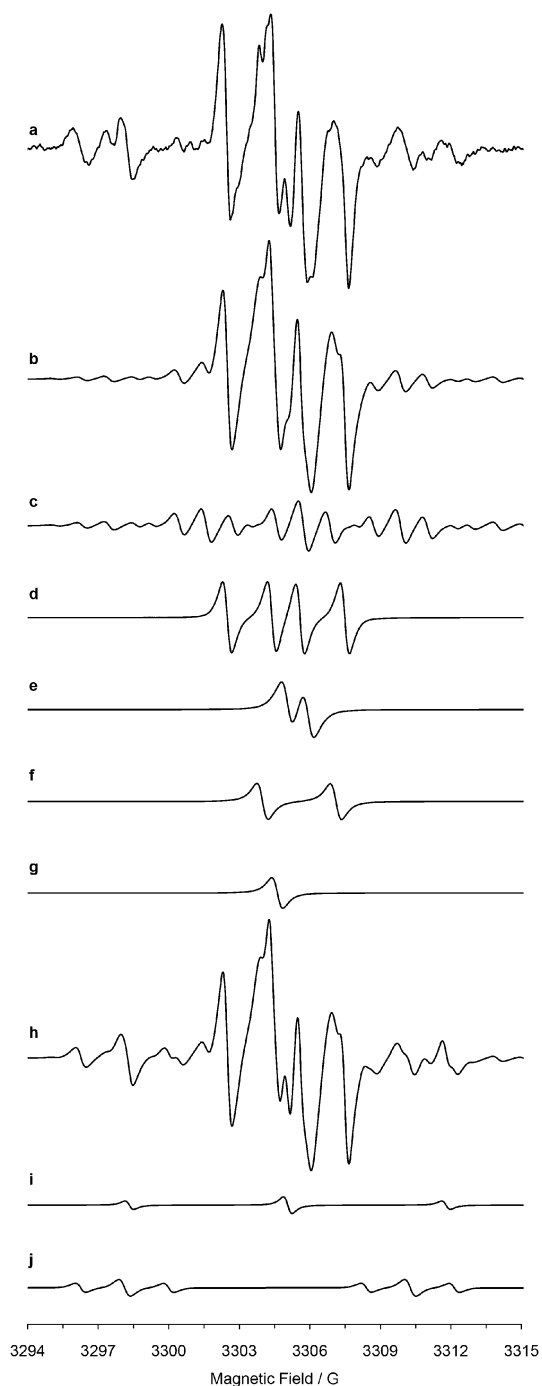


**Fig. 6** (a) Experimental EPR spectrum of 2 mM **C** in the presence of 85 mM H$_2$O$_2$ at pH = 12 and at a flow rate of 55 ml h$^{-1}$ (**C** + H$_2$O$_2$ (pH = 12) in Fig. 4. (b) Superposition of the radicals **C-1** to **C-5**. Simulation of (c) **C-1** (18%); (d) **C-2** (26%); (e) **C-3** (20%); (f) **C-4** (13%); (g) **C-5** (11%); (h) Superposition of the radicals **C-1** to **C-7**. Simulation of (i) **C-6** (6%); (j) **C-7** (6%).

existence of the two additional species **C-6** and **C-7** (*cf.* Fig. 6h–j). The formation of **C-6** and **C-7** would further be understandable from a chemical point of view. Their formation and also that of **C-1** to **C-5** cannot be explained by the addition of superoxide radical anions according to Fig. 7 or of singlet oxygen according to Fig. 8 as reported in

**Table 3** Experimental and calculated (B3LYP/6-31G(d)//B3LYP/EPR-III) EPR parameter of the radicals formed in the reaction of **C** with $H_2O_2$ under UV irradiation; R = $C_6F_4O^-$

| hfcc [G] from | | | |
|---|---|---|---|
| Simulation | DFT | g-factor | Proposed structure |
| 4 F (3,3′,5,5′): 4.13<br>4 F (2,2′,6,6′): 1.14 | 4 F (3,3′,5,5′): 5.57<br>4 F (2,2′,6,6′): 2.00 | 2.0061 | **C-1** (18%) |
| 1 F (3): 3.10<br>1 F (6): 1.90 | 1 F (3): 2.84<br>1 F (6): 1.92 | 2.0066 | **C-2** (26%) |
| 1 F (5): 0.88 | 1 F (5): 0.39 | 2.0062 | **C-3** (20%) |
| 1 F (6): 3.12 | 1 F (6): 5.80 | 2.0062 | **C-4** (13%) |
| | | 2.0068 | **C-5** (11%) |
| 2 F (2,6): 6.73 | 2 F (2,6): 4.78 | 2.0065 | **C-6** (6%) |
| 1 F (6): 12.14<br>1 F (2): 1.94<br>1 F (5): 1.80 | 1 F (6): 6.74<br>1 F (2): 2.97<br>1 F (5): 0.62 | 2.0070 | **C-7** (6%) |

the literature for nonfluorinated radicals. The latter two reaction mechanisms pass through keto-enol tautomerisms which require the presence of $C_{ar}$–H bonds (with $C_{ar}$ = aromatic carbon atom). However, the perfluorinated model compound **C** has only $C_{ar}$–F bonds. As the oxygen radical anion ($O^{\bullet-}$) is significantly less electrophilic than the hydroxyl radical ($HO^\bullet$), but is in excess at pH > $pK_a(HO^\bullet/O^{\bullet-})$ = 11.5, an alternative mechanism according to Fig. 9 is conceivable. In the first reaction step, the phenoxyl radical **C-1** is formed by one-electron oxidation of the corresponding bisphenolate by $O^{\bullet-}$ and $HO^\bullet$ radicals, respectively. The remaining fluorine atoms of **C-1** can then be substituted by $HO^-$ in highly alkaline solution. Such $S_NAr$ reactions, for example, serve for the synthesis of the model compound **C** from decafluorobiphenyl[76] and are known from degradation reactions of perchlorinated aromatics.[77]
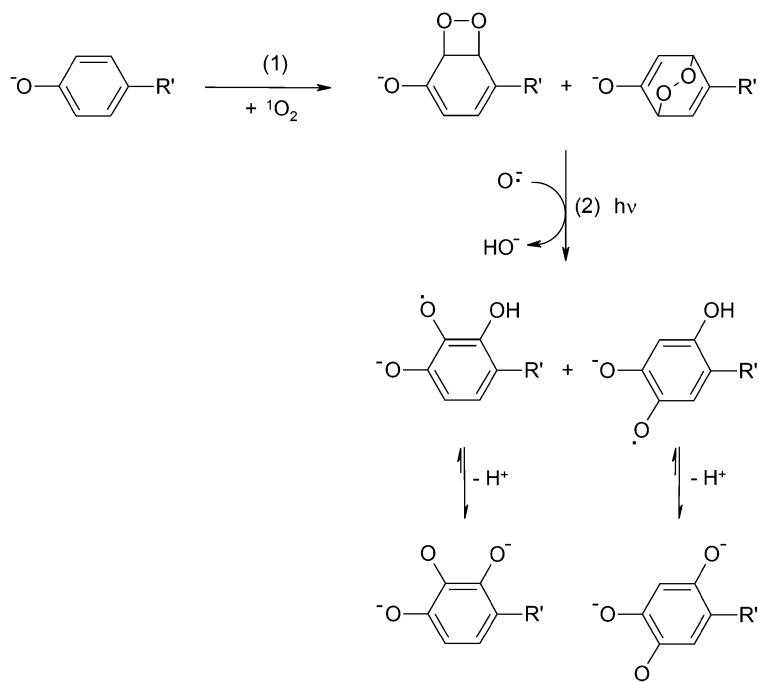
### 3.5 4,4′-Thiodiphenol (D)

4,4′-Thiodiphenol (**D**) causes EPR signals both in the presence and in the absence of hydrogen peroxide at high pH values (pH = 12) and low flow rates (8 ml h$^{-1}$); the spectra are shown in Fig. 10. In the absence of hydrogen peroxide (under UV irradiation) a triplet (g = 2.0051 G, a = 0.90 G) can be observed which also contributes to the superposition of the simulated radicals in the presence of hydrogen peroxide (**D-4**; Fig. 11 and Table 5). 4-Oxidophenyl- and (4-oxidophenyl)-sulfanyl (Table 4) radicals could be formed by photolytic cleavage of the weakest (C–S) bond in the molecule. Their EPR spectra could eventually suggest a triplet if the hyperfine interaction to the protons H-3 and H-5 was sufficiently small not be resolved.

As the values in Table 4 prove, this photochemical reaction can be excluded. However, the observed triplet could be explained by the radical **D-4** (*cf*. Table 5). The formation of similar oxidosubstituted benzosemiquinone radicals has been observed in previous investigations,[4,54,62] but the proposed reaction mechanism can only occur in the presence of photons and $O_2^{\bullet-}$ radicals or $^1O_2$ (*cf*. Fig. 7 and 8). In principle, the observed radicals **D-2** to **D-6** could be formed by such a mechanism; however, the origin of radical **D-4** under $H_2O_2$-free conditions cannot be traced back on this reaction pathway.

A possible explanation is given in Fig. 12. Photoexcited 4,4′-thiodiphenol molecules can ionize into the corresponding phenoxyl radicals and hydrated electrons.[79–87] The lifetime of these hydrated electrons is mainly limited by reaction m (Table 6) which might explain the lack of EPR signals of the free electron.[88] Table 6 further lists the reaction rate of phenol with hydrated electrons as the value for 4,4′-thiodiphenol could not be found in the literature, but the latter is expected to be in the same order of magnitude. The possible reaction of hydrated electrons with the cosolvent methanol can be excluded as well, as the rate constant is lower by several orders of magnitude. The primarily formed phenoxyl radicals (from reaction step (2) in Fig. 12) could not be detected by EPR spectroscopy (a = 2.13 G (4 H)),[89] which might be traced back to a low concentration and/or short lifetime. The reason for this could be the univalent dehydrogenation of water by

5788 | *Phys. Chem. Chem. Phys.*, 2009, **11**, 5782–5795

This journal is © the Owner Societies 2009
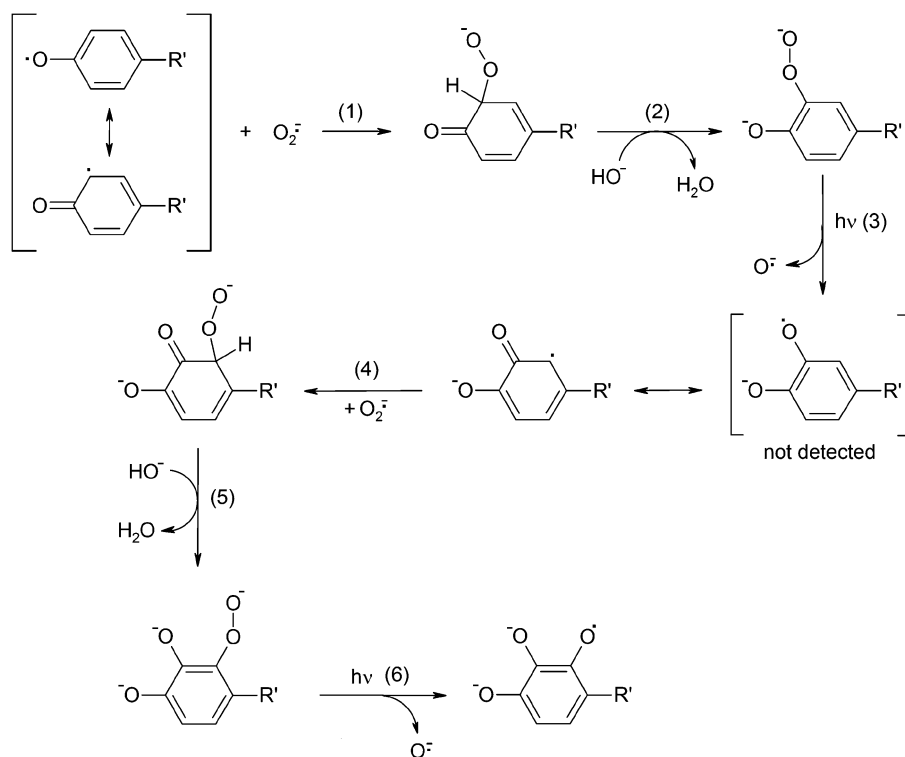
**Fig. 7** Proposed reaction mechanism for the formation of oxidosubstituted benzosemiquinone radicals in the presence of superoxide radical anions under UV irradiation.[54]
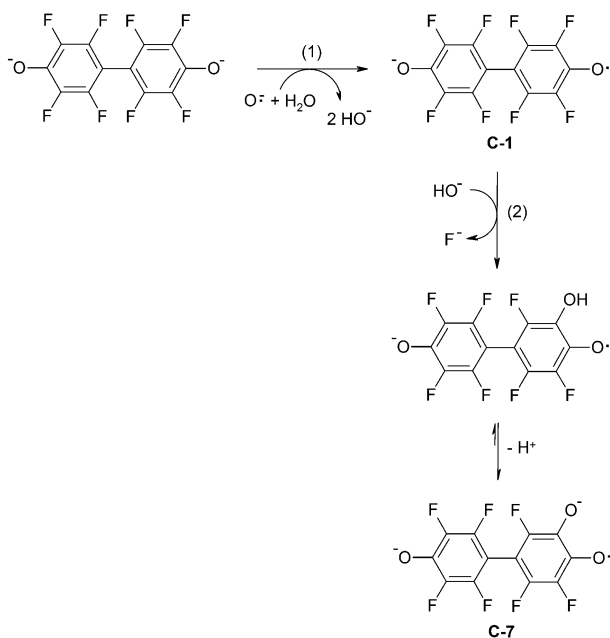
**Fig. 8** Proposed reaction mechanism for the formation of oxidosubstituted benzosemiquinone radicals in the presence of singlet oxygen under UV irradiation.[54]

the formed phenoxyl radicals under the reformation of 4,4′-thiodiphenolate and the release of HO• radicals. Because of the released protons in the acid–base reactions (4) and (5), the initially adjusted pH value could slightly drop. These HO•

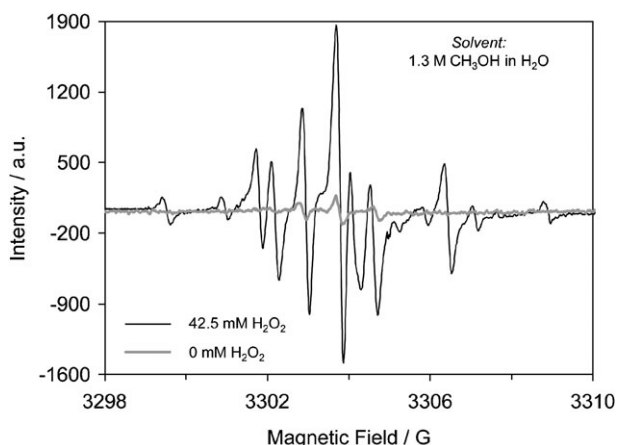and O•− radicals might be responsible for the formation of **D-4**, even under hydrogen peroxide free conditions.

Radical **D-1** has been detected in a previous study as degradation product of 2,2-bis(4-hydroxyphenyl)sulfone. Its
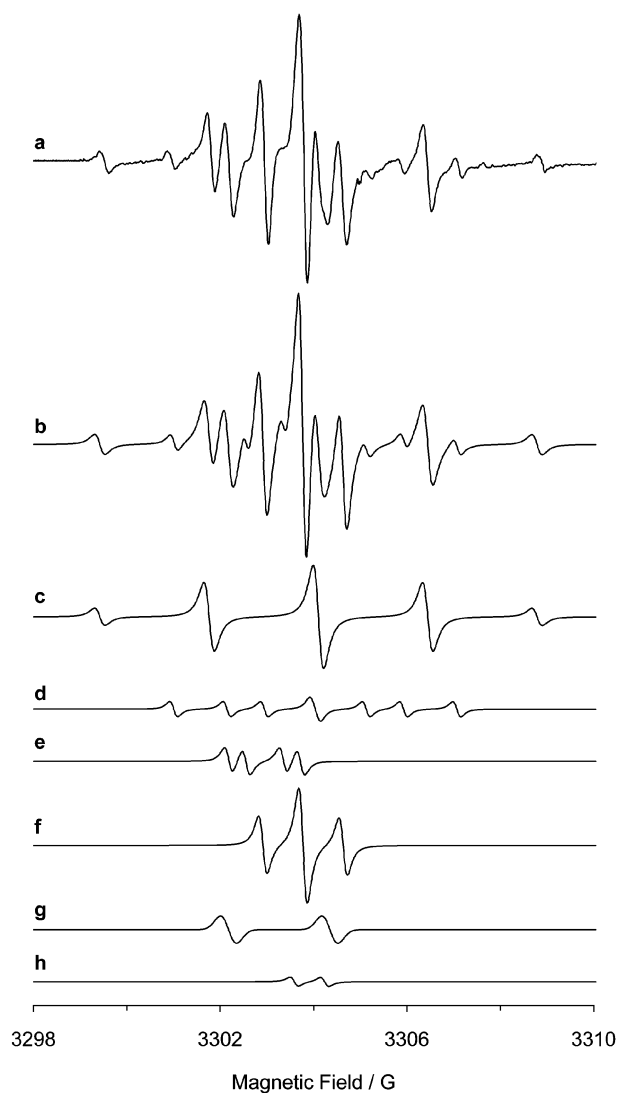
**Fig. 9** Possible reaction mechanism for the formation of the radicals **C-1** to **C-7** in alkaline medium.



**Fig. 10** EPR spectra of 4,4′-thiodiphenol (**D**) in the presence and absence of hydrogen peroxide (conditions: 6.4 mM **D**; pH = 12; flow rate 8 ml h$^{-1}$) in aqueous methanol solution (1.3 M CH$_3$OH).



**Fig. 11** (a) Experimental EPR spectrum of **D** in the presence of hydrogen peroxide at pH = 12 and with a flow rate of 8 ml h$^{-1}$ (measured in 1.3 M CH$_3$OH in H$_2$O). (b) Superposition of simulations of the radicals **D-1** to **D-6**. Simulation of (c) **D-1** (34%); (d) **D-2** (8%); (e) **D-3** (9%); (f) **D-4** (38%); **D-5** (8%) and (h) **D-6** (3%).
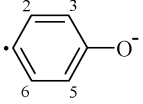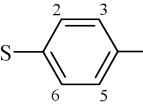
formation could be initiated by the addition of a HO$^\bullet$ radical to the aromatic carbon next to the sulfur atom (reaction step (1) in Fig. 13). The subsequent deprotonation (2) under the basic conditions favors the elimination of 4-sulfidophenolate (3) by the enhanced +M effect of the oxido substituent. According to Table 5, an increase in the flow rate at a constant pH value of 12 particularly influences the ratio of the radicals **D-1** and **D-6**. The intensity of the signal caused by **D-1** decreases, while that caused by **D-6** increases. An explicit explanation for it cannot be given here, but it might be possible that the addition of HO$^\bullet$ radicals at the carbon next to the sulfur atom is kinetically more hindered than the formation of phenoxyl radicals which serve for the reaction cascade in Fig. 7. The intensities of the other radicals **D-2** to **D-5** do not seem to be influenced significantly by the flow rate.

**D-6** only contributes by 3% at low flow rate (8 ml h$^{-1}$) while it contributes by 9% to the simulation at high flow rate (150 ml h$^{-1}$). One should expect at first look that **D-6** would be a secondary radical formed from **D-2**, **D-3** and **D-4**, respectively. It should thus be observed in higher amounts at low flow rates, which is obviously not the case. Providing the radical structure assignments are correct, this would mean that **D-6** is not derived from **D-2**, **D-3** and **D-4**, respectively. This could further suggest that the formation of **D-2** to **D-5** on the one hand and the formation of **D-6** on the other hand proceed *via* competing reactions. However, no mechanistic details can be given here. In the last part of this section, the radical composition will be examined with dependence on the pH value. While no EPR signals could be detected below pH = 10.2 (Fig. 14), there is a more or less pronounced pH dependence of the intensity ratio in the range 10.5 < pH < 13.2 (Fig. 15). Especially at very high pH values

**Table 4** EPR parameters of 4-oxidophenyl- and (4-oxidophenyl)-sulfanyl radicals (calculated by Gaussian 03 and taken from the literature if available)

| hfcc [G] | g-Factor | Radical structure |
|---|---|---|
| 2 H (3,5): 5.96 G$^a$ (4.90 G)[78] | 2.00226[78] | 4-Oxidophenyl radical |
| 2 H (2,6): 0.60 G$^b$ (0.40 G)$^c$ <br> 2 H (3,5): 2.35 G$^b$ (3.14 G)$^c$ | | (4-Oxidophenyl)sulfanyl radical |

$^a$ B3LYP/6-31G(d)//B3LYP/EPR-III. $^b$ B3LYP/TZVP//B3LYP/TZVP. $^c$ B3LYP/6-31G(d)//B3LYP/6-31G(d).
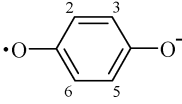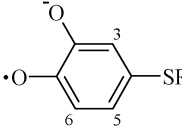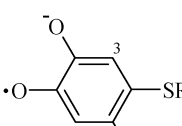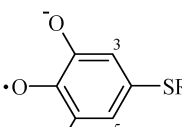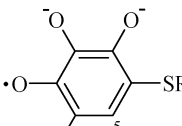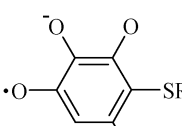
(pH = 13.2) the percentage of the *p*-benzosemiquinone radical **D-1** and of the lower oxidosubstituted radicals **D-2** and **D-3** decreases for the benefit of the higher oxidosubstituted ones **D-4** to **D-6**.

At pH > 13 the radicals O$^{\bullet-}$ and O$_2^{\bullet-}$ are prevalent while a complex mixture of HO$^\bullet$, O$^{\bullet-}$ and O$_2^{\bullet-}$ exists in the range 10 ≤ pH ≤ 13. Caused by the higher concentration of O$_2^{\bullet-}$ at pH = 13.2, the probability of a bimolecular collision with an already hydroxylated species (*e.g.* reaction steps (1) and (4) in Fig. 7) is higher. The composition at pH = 12 is essentially determined by the radicals **D-1** and **D-4**. The percentage of the higher hydroxylated radicals **D-5** and **D-6** in the superposition of the various radicals at pH = 10.5 is relatively high. However, the molecular process responsible for this could not be clarified on the basis of the data presented.

### 3.6 Comparison between the various model compounds

The model compounds were chosen in such a way that they represent different C–F bond types: C$_{sp3}$–F in the model compounds **A** and **B**, C$_{sp2}$–F in the model compound **C**. All model compounds yield phenoxyl and benzosemiquinone radicals at slightly to strongly alkaline pH values under the chosen reaction conditions. As the conditions for obtaining analyzable EPR signals had to be adapted individually, a quantitative comparison cannot be made here. It can be stated that phenoxyl and benzosemiquinone radicals at elevated pH values are formed independently of the type and number of C–F bonds. In case of C$_{sp2}$–F bonds (as in the model compound **C**) the fluorine atoms might be substituted by oxido substituents. Because of the lower tendency of O$^{\bullet-}$ for an electrophilic attack to arenes in comparison to that of HO$^\bullet$, the following mechanism seems likely. After one-electron oxidation by O$^{\bullet-}$, a perfluorinated phenoxyl radical is formed whose fluorine atoms might subsequently be exchanged by HO$^-$ in the alkaline medium. However, if C$_{sp3}$–F bonds are present in the model compound (like in **B**) they do not seem to be attacked. It might also be interesting for any further polymer and ionomer development to note that the sulfonated model compound **B** yields a phenoxyl radical already at pH = 7.3 (and most probably already at pH = 5.3). On the

**Table 5** Experimental and calculated EPR parameter of the radicals formed in the reaction of **D** with H$_2$O$_2$ under UV irradiation (pH = 12, flow rate 8 ml h$^{-1}$); R = C$_6$H$_3$(*m*-SO$_3^-$)(*p*-O$^-$)

| hfcc [G] from Simulation (literature)$^a$ | DFT$^b$ | g-Factor | Proposed structure |
|---|---|---|---|
| 4 H (2,3,5,6): 2.34 (2.35) | 4 H (2,3,5,6): 2.32 calculated with b3lyp/6-31G(d)// b3lyp/epr-iii | 2.0049 | **D-1** <br> 34% at 8 ml h$^{-1}$ <br> 25% at 150 ml h$^{-1}$ |
| 1 H (3): 1.14 <br> 1 H (5): 1.94 <br> 1 H (6): 2.98 | 1 H (3): 1.04 <br> 1 H (5): 2.56 <br> 1 H (6): 3.18 | 2.0049 | **D-2** <br> 8% at 8 ml h$^{-1}$ <br> 7% at 150 ml h$^{-1}$ |
| 1 H (3): 1.17 <br> 1 H (6): 0.37 | 1 H (3): 1.06 <br> 1 H (6): 0.38 | 2.0056 | **D-3** <br> 9% at 8 ml h$^{-1}$ <br> 9% at 150 ml h$^{-1}$ |
| 2 H (3,5): 0.86 | 2 H (3,5): 1.26 | 2.0051 | **D-4** <br> 38% at 8 ml h$^{-1}$ <br> 41% at 150 ml h$^{-1}$ |
| 1 H (5): 2.17 | 1 H (5): 1.52 | 2.0054 | **D-5** <br> 8% at 8 ml h$^{-1}$ <br> 9% at 150 ml h$^{-1}$ |
| 1 H (6): 0.65 | 1 H (6): 0.32 | 2.0050 | **D-6** <br> 3% at 8 ml h$^{-1}$ <br> 9% at 150 ml h$^{-1}$ |

$^a$ If available. $^b$ Calculated with B3LYP/TZVP//B3LYP/TZVP (Gaussian 03) if not otherwise stated.
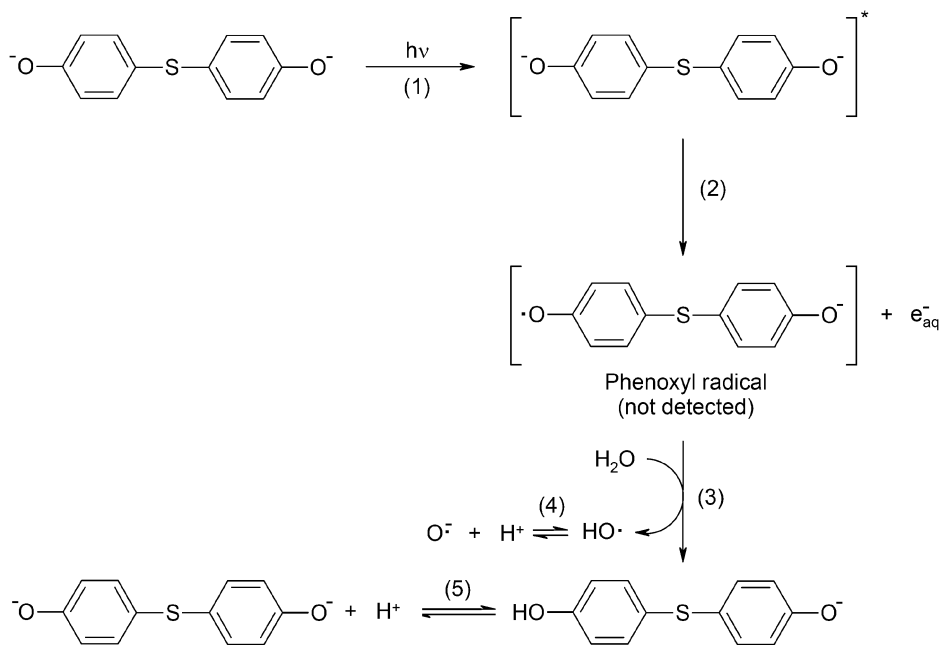
**Fig. 12** Formation of hydroxyl radicals and hydrated electrons by photoionisation of 4,4′-thiodiphenol.

**Table 6** Overview of possible reactions and their reaction rates of hydrated electrons[55]

|   | pH | Reaction | Rate constant/ $10^9$ $M^{-1}$ $s^{-1}$ |
|---|---|---|---|
| k |  | $e^-_{aq} + CH_3OH \rightarrow H^{\bullet} + CH_3O^-$ | $<0.00001$ |
| l | 11 | $e^-_{aq} + C_6H_5O^- \rightarrow C_6H_5O^{2-}$ | 0.004 |
| m | 11–13 | $e^-_{aq} + e^-_{aq} + 2\,H_2O \rightarrow H_2 + 2\,HO^-$ | 5.0 |

other hand, the nonsulfonated model compounds **A**, **C** and **D** form phenoxyl and benzosemiquinone radicals only at higher

pH values. Although differences in the concentration might be jointly responsible for the observed pH dependency, it is likely that a six-membered transition state between the hydroxyl and sulfonic acid group could facilitate the formation of the corresponding phenoxyl radicals in the case of the sulfonated model compound **B**.

In the case of the aqueous-methanolic test solutions (**A**, **C** and **D**), no evidence for the formation of methylol radicals (according to reactions d and f in Table 1) could be found. Considering the difference in concentrations for the various monomers and for methanol (Table 7), one can
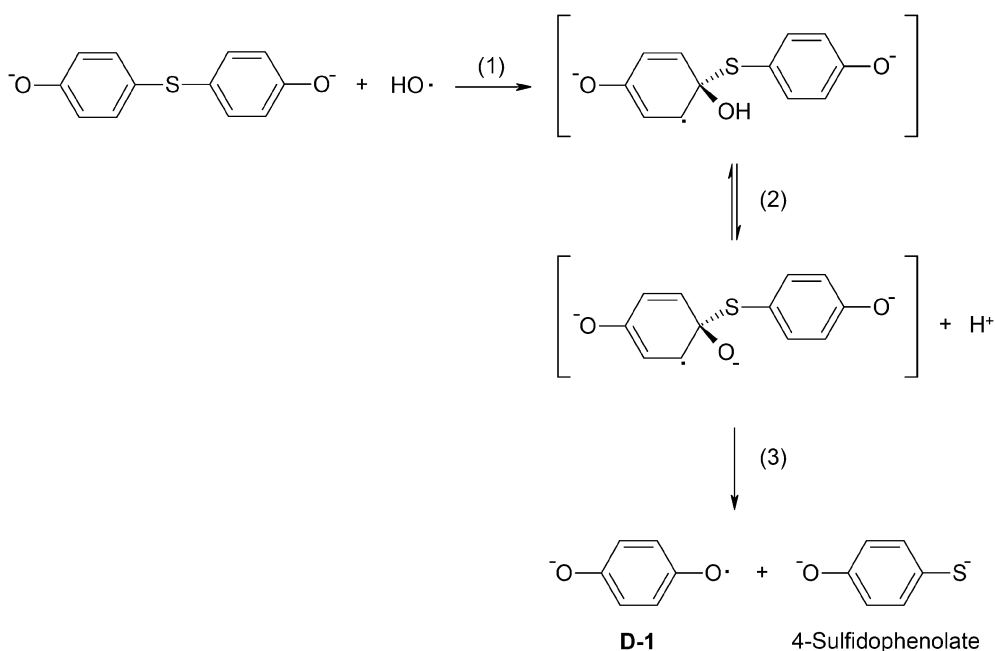
**Fig. 13** Possible reaction mechanism for the formation of the *p*-benzosemiquinone radicals **D-1**.
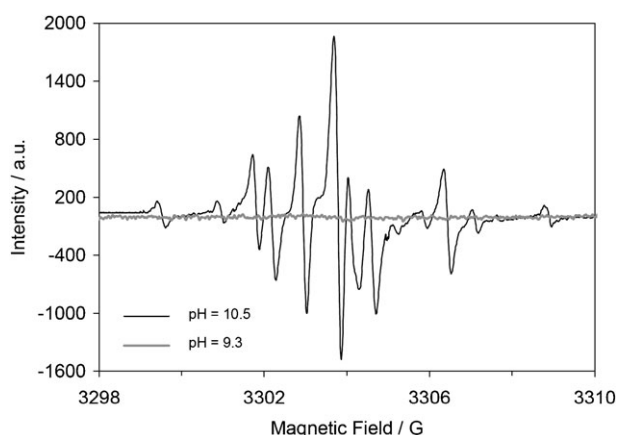
Fig. 14 Dependence of the EPR signals from the pH value (conditions: 6.4 mM **D**; 42.5 mM $H_2O_2$; flow rate: 8 ml h$^{-1}$; 1.3 M $CH_3OH$). As no signals could be detected at pH values below 10.2, only the EPR spectrum at pH = 9.3 is depicted in this diagram to represent the lower pH range.



Fig. 15 Radical composition of the solution in dependence of the pH value.

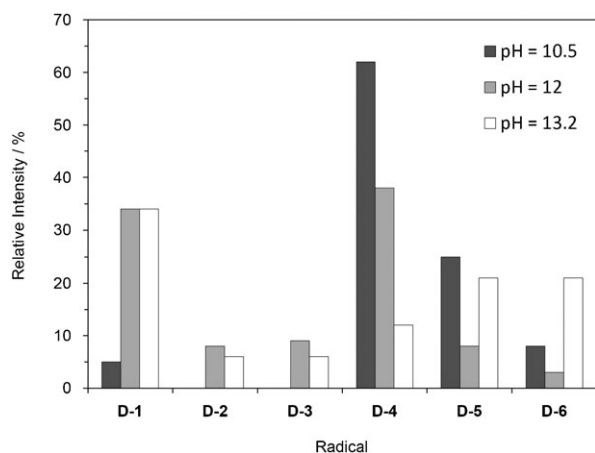Table 7 Overview of the investigated model compounds **A** to **D** and of the pH range in which radicals of the phenoxyl and benzosemi-quinone type could be observed

| Model compound | Concentration monomer/ $CH_3OH$ ($H_2O_2$)/mM | Flow rate/ ml h$^{-1}$ | pH range |
|---|---|---|---|
| **A**[a] | 3.2/1300 (170) | 8 | ≈12 |
| **B** | 12.8/0 (85) | 35 | (5.3) 7.3–11.4 |
| **C** | 2.0/4400 (85) | 35 | 11.2–14.0 |
| **D** | 6.4/1300 (42.5) | 8–150 | 10.5–13.2 |

[a] Complex reaction mixture, oscillating radical concentration.

conclude a significantly preferred reactivity of HO• and related radicals with the aromatic model compounds than with the competing methanol solvent.

## Conclusions

Reactions between monomeric model compounds (representing typical structure moieties of poly(aryl) ionomers) and $H_2O_2$ in

aqueous(-methanolic) solution under UV irradation have been examined within the cavity of an EPR spectrometer.

As the reaction conditions in the test solution are not comparable in every respect to those in a working fuel cell, a critical analysis is necessary. Due to the chosen experimental setup for the generation of HO• radicals, it cannot be excluded that the high-energy UV radiation causes any photophysical processes or photochemical reactions of the tested monomer directly. Beside the excitation into a higher electronic state from which any reaction with other species could be facilitated,[61] a direct photochemical dissociation (such as the cleavage-off of the •$SO_3^-$ radical in case of the model compound **B**) or a photoionization (as in the case of **D**) are worth mentioning. Such photoinduced processes—which play an important role in the ageing and degradation of polymers in general[90]—are not relevant for membrane degradation within a fuel cell stack. However, the sulfonic acid group of the aromatic model compound does not seem to react with HO• radicals under the chosen conditions.

A further difference between the test solution and the fuel cell membrane lies in their chemical composition (monomer in the first case, polymer in the second case) and in their physical state (solution or multiphase system, respectively). This means that every model compound possesses two functional groups (e.g. hydroxyl groups) while there are only two functional end-groups per poly(aryl) ionomer. However, the importance of end-groups for the HO• radical induced degradation should not be underestimated as was shown earlier for the example of poly(perfluorosulfonic aicd).[13,91] Furthermore, HO• radical[4] or acid[2] induced ether cleavages can enhance the number of potential end groups in the case of sulfonated poly(arylene ether)s.

Another aspect of this discussion concerns the pH value of the test solutions in comparison to that in a real polymer electrolyte membrane. Most of the identified radicals could be observed only at elevated pH values. This does not necessarily mean that no radicals are formed at lower pH values, but their concentration could be below the detection limit (especially in case of short-lived radicals).[63] Indications for any kind of reaction (such as colour change, gas evolution) could be observed for all the investigated model compounds at various pH values so that some reaction (not necessarily a radical-involved one) is likely.

The pH value in a swollen proton-exchange membrane is in the range of pH ≈ 0. During fuel cell operation local pH inhomogeneities could arise close to the catalyst particles especially under high loading.[18] These inhomogeneities could then induce the same or similar reactions as those presented in this paper. In addition, the presented model compounds might also be relevant as building blocks for alkaline anion-exchange membrane fuel cells (AAEMFCs)[92,93] which naturally work at pH ≈ 14. This type of fuel cell could be of interest for future research because the electrode kinetics are faster in an alkaline medium[94] which allows the use of platinum-free catalysts.[95]

The reaction conditions applied for the investigation of these model compounds are therefore not completely comparable to those in a working fuel cell. However, the following conclusions for further polymer and ionomer development may be drawn:

• Alkaline conditions facilitate the formation of phenoxyl and benzosemiquinone radicals, *i.e.* local inhomogeneities in pH should be avoided when such building blocks are present. The application of such aromatic building blocks in alkaline–anion exchange membrane fuel cells holds the risk of an enhanced susceptibility to HO[•] and related radicals, especially when hydroxyl end-groups are present.

• The number of potentially reactive end-groups (especially of hydroxyl groups and fluorine atoms) should be minimized (*e.g.* by endcapping of the polymers with a monofunctional aromatic monomer).

• The ether bridge of poly(arylene ether)s has to be stabilized against HO[•] radical, acid or base induced cleavage by appropriate electron-withdrawing substituent in *ortho*- or *para*-position in order to reduce the probability of chain cleavage during fuel cell operation.[32] Any cleaved ether bridges might activate a cascade of (further) radical induced reactions (especially in a locally alkaline medium).

## Acknowledgements

## References

1 L. Zhang and S. Mukerjee, *J. Electrochem. Soc.*, 2000, **153**(6), A1062.
2 J. Kerres and F. Schönberger, *Fundamental Aspects of Membrane Degradation*, International Workshop on Degradation Issues in Fuel Cells, Hersonissos, Crete, (Greece), September 19th–21st, 2007.
3 N. Ramaswamy, N. Hakim and S. Mukerjee, *Electrochim. Acta*, 2008, **53**, 3279.
4 G. Hübner and E. Roduner, *J. Mater. Chem.*, 1999, **9**, 409.
5 A. Panchenko, H. Dilger, E. Möller, T. Sixt and E. Roduner, *J. Power Sources*, 2004, **127**, 325.
6 A. Panchenko, H. Dilger, J. Kerres, M. Hein, A. Ullrich, T. Kaz and E. Roduner, *Phys. Chem. Chem. Phys.*, 2004, **6**, 2891.
7 A. Panchenko, *J. Membr. Sci.*, 2006, **278**(1–2), 269.
8 S. Mitov, O. Delmer, J. Kerres and E. Roduner, *Helv. Chim. Acta*, 2006, **89**, 2354.
9 A. B. Anderson and T. V. Albu, *J. Electrochem. Soc.*, 2000, **147**(1), 4229.
10 U. A. Paulus, T. J. Schmidt, H. A. Gasteiger and R. J. Behm, *J. Electroanal. Chem.*, 2001, **492**, 134.
11 V. O. Mittal, H. R. Kunz and J. M. Fenton, *Electrochem. Solid States*, 2006, **9**(6), A299.
12 S. Mitov, B. Vogel, E. Roduner, H. Zhang, X. Zhu, V. Gogel, L. Jörissen, M. Hein, D. Xing, F. Schönberger and J. Kerres, *Fuel Cells*, 2006, **6**, 413.
13 D. E. Curtin, R. D. Lousenberg, T. J. Henry, P. C. Tangeman and M. E. Tisack, *J. Power Sources*, 2004, **131**, 41.
14 M. Danilczuk, F. D. Coms and S. Schlick, *Fuel Cells*, 2008, **8**(6), 436.
15 C. Zhou, M. A. Guerra, Z.-M. Qiu, T. A. Zawodzinski and D. A. Schiraldi, *Macromolecules*, 2007, **40**(24), 8695.
16 E. Roduner and S. Schlick, ESR Methods for Assessing the Stabiltiy of Polymer Membranes Used in Fuel Cells, in *Advanced ESR Methods in Polymer Research*, ed. S. Schlick, John Wiley & Sons, 2006, ch. 8.
17 B. Vogel, E. Aleksandrova, S. Mito, M. Krafft, A. Dreizler, J. Kerres, M. Hein and E. Roduner, *J. Electrochem. Soc.*, 2008, **155**(6), B570.
18 A. Bosnjakovic and S. Schlick, *J. Phys. Chem. B*, 2004, **108**, 4332.
19 H. C. Lee, H. S. Hong, Y.-M. Kim, S. H. Choi, M. Z. Hong, H. S. Lee and K. Kim, *Electrochim. Acta*, 2004, **49**, 2315.
20 J. A. Kerres, D. Xing and F. Schönberger, *J. Polym. Sci., Part B: Polym. Phys.*, 2006, **44**(16), 2311.
21 C. Hamiciuc, M. Bruma and M. Kapper, *J. Macromol. Sci. A*, 2001, **38**(7), 659.
22 P. Xing, G. P. Robertson, M. D. Guiver, S. D. Mikhailenko and S. Kaliaguine, *Macromolecules*, 2004, **37**, 7960.
23 B. Liu, G. P. Robertson, M. D. Guiver, Y.-M. Sun, Y.-L. Liu, J.-Y. Lai, S. Mikhailenko and S. Kaliaguine, *J. Polym. Sci., Part B: Polym. Phys.*, 2006, **44**, 2299.
24 W. L. Harrison, F. Wang, J. B. Mecham, V. A. Bhanu, M. Hill, Y. S. Kim and J. E. McGrath, *J. Polym. Sci., Part A: Polym. Chem.*, 2003, **41**, 2264.
25 F. Schönberger, M. Hein and J. Kerres, *Solid State Ionics*, 2007, **178**, 547.
26 N. Y. Arnett, W. L. Harrison, A. S. Badami, A. Roy, O. Lane, F. Cromer, L. Dong and J. E. McGrath, *J. Power Sources*, 2007, **172**, 20.
27 K. B. Wiles, C. M. de Diego, J. de Abajo and J. E. McGrath, *J. Membr. Sci.*, 2007, **294**, 22.
28 Z. Bai, J. A. Shumaker, T. D. Dang, M. Yoonessi and M. F. Durstock, *Polym. Preprints*, 2006, **47**(1), 140.
29 Y. S. Kim, M. J. Sumner, W. L. Harrison, J. S. Riffle, J. E. McGrath and B. S. Pivovar, *J. Electrochem. Soc.*, 2004, **151**(12), A2150.
30 M. Sankir, Y. S. Kim, B. S. Pivovar and J. E. McGrath, *J. Membr. Sci.*, 2007, **299**, 8.
31 T. L. Norsten, M. D. Guiver, J. Murphy, T. Astill, T. Navessin, S. Holdcroft, B. L. Frankamp, V. M. Rotello and J. Ding, *Adv. Funct. Mater.*, 2006, **16**, 1814.
32 F. Schönberger, A. Chromik and J. Kerres, *Polymer*, 2009, **50**, 2010.
33 Z. Bai, M. F. Durstock and T. D. Dang, *J. Membr. Sci.*, 2006, **281**, 508.
34 Z. Bai and T. D. Dang, *Macromol. Rapid Commun.*, 2006, **27**, 1271.
35 J. K. Lee and J. Kerres, *J. Membr. Sci.*, 2006, **294**, 75.
36 G. Xiao, G. Sun and D. Yan, *Polym. Preprints*, 2003, **44**(1), 1235.
37 M. Schuster, K.-D. Kreuer, H. T. Anderson and J. Maier, *Macromolecules*, 2007, **40**, 598.
38 WINSIM[®], National Institute of Environmental Health Science, http://www.niehs.nih.gov.
39 Landolt-Börnstein, Group II: Molecules and Radicals, Springer-Verlag, 2006.
40 http://www.gaussian.com.
41 H. Haken and H. C. Wolf, *Molekülphysik und Quantenchemie, 5. Auflage*, Springer Verlag, 2006.
42 L. Hermosilla, P. Calle, J. M. García de la Vega and C. Sieiro, *J. Phys. Chem. A*, 2005, **109**, 1114.
43 B. T. Nguyen, S. Creve, L. A. Eriksson and L. A. Vanquickenborne, *Mol. Phys.*, 1997, **91**(3), 537.
44 T. H. Dunning, Jr, *J. Chem. Phys.*, 1989, **90**(2), 1007.
45 N. Rega, M. Cossi and V. Barone, *J. Chem. Phys.*, 1996, **105**(24), 11060.
46 C. Adamo, V. Barone and A. Fortunelli, *J. Phys. Chem.*, 1994, **98**, 8648.
47 P. A. M. Dirac, *Proc. R. Soc. London, Ser. A*, 1929, **123**, 714.
48 J. C. Slater, *Phys. Rev. A*, 1951, **81**, 385.
49 S. H. Vosko, L. Wilk and M. Nusair, *Can. J. Phys.*, 1980, **58**, 1200.
50 A. D. Becke, *Phys. Rev. A*, 1988, **38**, 3098.
51 C. Lee, W. Yang and R. G. Parr, *Phys. Rev. B*, 1988, **37**, 785.
52 A. D. Becke, *J. Chem. Phys.*, 1993, **98**, 5648.
53 A. R. Rakitin, D. Yff and C. Trapp, *J. Phys. Chem. A*, 2003, **107**, 6281.
54 S. Mitov, PhD Thesis, University of Stuttgart, 2007.
55 G. V. Buxton, C. L. Greenstock, W. P. Helman and A. B. Boss, *J. Phys. Chem. Ref. Data*, 1988, **17**(2), 513.
56 B. H. J. Bielski, D. E. Cabelli, R. L. Arudi and A. B Boss, *J. Phys. Chem. Ref. Data*, 1985, **14**(4), 1985, 1041.
57 X.-Y. Yu and J. R. Barker, *J. Phys. Chem. A*, 2003, **107**, 1313.
58 K.-D. Asmus, H. Möckel and A. Heinglein, *J. Phys. Chem.*, 1973, **77**, 1218.
59 G. A. Poskrebyshev, P. Neta and R. E. Huie, *J. Phys. Chem. A*, 2002, **106**(47), 11488.
60 A. D. N. J. De Grey, *DNA Cell Biol.*, 2002, **21**(4), 251.
61 G. Wypych, *Handbook of Material Weathering*, ChemTec Publishing, 3rd edn, 2003.

62  G. Hübner, PhD Thesis, University of Stuttgart, 1999.
63  J. A. Weil, J. R. Bolton and J. E. Wertz, *Electron Paramagnetic Resonance*, John Wiley & Sons, 1994.
64  J. L. Ferry and M. A. Fox, *J. Phys. Chem. A*, 1998, **102**, 3705.
65  S. Steenken, *J. Chem. Soc., Faraday Trans. 1*, 1987, **83**, 113.
66  A. E. da Hora Machado, R. Ruggiero and M. G. Neumann, *J. Photochem. Photobiol., A*, 1994, **81**, 107.
67  E. A. Almeida, S. Miyamoto, G. R. Martinez, M. H. G. Medeiros and P. D. Mascio, *Anal. Chim. Acta*, 2003, **482**, 99.
68  T. Kajiwara and D. R. Kearns, *J. Am. Chem. Soc.*, 1973, **95**, 5886.
69  J. Feitelson and E. Hayon, *J. Phys. Chem.*, 1973, **77**(1), 10.
70  J. Pola, M. Urabnová, Z. Bastl, Z. Plzák, J. Šubrt, I. Gregora and V. Vorlíček, *J. Mater. Chem.*, 1998, **8**(1), 187.
71  P. W. Atkins, *Physikalische Chemie, 2. Auflage*, Wiley-VCH, 1996.
72  V. A. Benderskii, A. U. Goldschleger, A. V. Akimov, E. Y. Misochko and C. A. Wight, *Mendeleev Commun.*, 1996, **6**, 245.
73  J. Pola, M. Urbanová, Z. Bastl, Z. Plzák, J. Šubrt, I. Gregora and V. Vorlíček, *J. Mater. Chem.*, 1998, **8**(1), 187.
74  I. Haller, *J. Am. Chem. Soc.*, 1966, **88**, 2070.
75  G. Camaggi, F. Gozzo and G. Cevidalli, *Chem. Commun.*, 1996, 313.
76  D. J. Byron, A. S. Matharu, R. C. Wilson and J. W. Brown, *Mol. Cryst. Liq. Crys., A*, 1995, **258**, 95.
77  D. H. Sarr, C. Kazunga, M. J. Charles, J. G. Pavlovich and M. D. Aitken, *Environ. Sci. Technol.*, 1995, **29**, 2735.
78  H. Zemel and R. W. Fessenden, *J. Phys. Chem.*, 1975, **79**, 1419.
79  M. Cocivera, M. Tomkiewicz and A. Groen, *J. Am. Chem. Soc.*, 1972, **20**, 6598.
80  L. I. Grossweiner, G. W. Swenson and E. F. Zwicker, *Science*, 1963, **141**(3583), 805.
81  J. Feitelson and E. Hayon, *J. Phys. Chem.*, 1973, **77**(1), 10.
82  J. Feitelson, E. Hayon and A. Treinin, *J. Am. Chem. Soc.*, 1972, **95**(4), 1025.
83  G. Köhler, G. Kittel and N. Getoff, *J. Photochem.*, 1982, **18**, 19.
84  A. S. Jeevarajan and R. W. Fessenden, *J. Phys. Chem.*, 1992, **96**, 1520.
85  Y. Kajii and R. W. Fessenden, *Res. Chem. Intermed.*, 1999, **25**(6), 567.
86  A. Bussandri and H. v. Willigen, *J. Phys. Chem. A*, 2002, **106**, 1524.
87  A. Bussandri and H. v. Willigen, *J. Phys. Chem. A*, 2001, **105**, 4669.
88  G. Brunton, B. C. Gilbert and R. J. Mawby, *J. Chem. Soc., Perkin Trans. 2*, 1976, **11**, 1297.
89  G. Brunton, B. C. Gilbert and R. J. Mawby, *J. Chem. Soc., Perkin Trans. 2*, 1976, **11**, 1297.
90  D. M. Wiles, *Polym. Eng. Sci.*, 1973, **13**(1), 74.
91  T. Kallio, K. Jokela, H. Ericson, R. Serimaa, G. Sundholm, P. Jacobsson and F. Sundholm, *J. Appl. Electrochem.*, 2003, **33**, 505.
92  J. R. Varcoe, R. C. T. Slade and E. L. H. Yee, *Chem. Commun.*, 2006, 1428.
93  J. R. Varcoe and R. C. T. Slade, *Fuel Cells*, 2005, **5**(2), 187.
94  G. F. McLean, T. Niet, S. Prince-Richard and N. Djilali, *Int. J. Hydrogen Energ.*, 2002, **27**, 507.
95  H. Meng and P. K. Shen, *Electrochem. Commun.*, 2006, **8**(4), 588.

This journal is © the Owner Societies 2009

*Phys. Chem. Chem. Phys.*, 2009, **11**, 5782–5795 | 5795